PERGAMON

International Journal of Heat and Mass Transfer 42 (1999) 1969–1978

International Journal of HEAT and MASS TRANSFER

An inverse method for estimation of the initial temperature profile and its evolution in polymer processing

K.T. Nguyen[a,*], M. Prystay[b]

[a] *Industrial Materials Institute, Boucherville, Quebec, Canada J4B 6Y4*
[b] *Oerlikon Aerospace Inc., St Jean sur Richelieu, Quebec, Canada J3B 8E9*

Received 14 April 1998; in final form 27 August 1998

Abstract

An inversion technique is developed to reconstruct the temperature distribution over the thickness of a part during polymer processing using the surface temperature measurement. The algorithm is validated using surface temperature data generated numerically from a number of theoretical temperature profiles developed during polymer flows. The technique is then applied to the injection stretch blow molding process. In this process a preform is injection molded, stretched to its final length and then inflated. A single stage AOKI machine is used for the experiments. An infrared camera is employed to measure the surface temperature of the preform with time after it is taken out of the injection mold. The initial temperature distribution in the preform and its temperature evolution before stretching and inflation are predicted.

Nomenclature

C_p specific heat [J kg^{-1} K^{-1}]
d half thickness of the part [mm]
$f(x)$ initial temperature profile
$\Delta f(x)$ variation in initial temperature profile
h heat transfer coefficient [W m^{-2} K^{-1}]
J functional to be minimized
J'^n gradient of J at iteration n
k thermal conductivity [W m^{-1} K^{-1}]
P^n direction of descent at iteration n
t time [s]
t_f final time
T temperature [°C]
T_a ambient temperature [°C]
$T_m(t)$ measured surface temperature with time [°C]
$T_s(t)$ computed surface temperature with time [°C]
x spatial coordinate in thickness direction [mm].

Greek symbols
α thermal diffusivity
β^n step size at iteration n
γ^n conjugate coefficient at iteration n
δ Dirac delta function
Θ sensitivity variable
ρ density [kg m^{-3}]
τ minimum time data required for the inversion
χ adjoint function of T.

1. Introduction

In polymer processes such as extrusion, injection molding or blow molding, the material undergoes a complex history in which it is melted, flows through complex geometries where viscous dissipation plays a central role, is deformed to take the shape of the mold, and finally is cooled down and solidified into the final product. Some typical examples of different polymer processes are described. Each example highlights the importance of temperature profiles for the optimization purposes.

In polymer extrusion, the material is plasticated in an extruder before passing through a die for shaping purpose. The material is usually assumed to have a constant temperature at the entrance of the die and the die is usually controlled at a given temperature. As such, it is hoped that the extrudate will have a uniform temperature. However, due to the history in the extruder, the

* Corresponding author. Tel.: 001 450 641 5066; fax: 001 450 641 5104; e-mail: ky.nguyen@nrc.ca

0017–9310/99/$ - see front matter
PII: S0017–9310(98)00297–X

material temperature at the die entrance is rarely uniform. It is difficult to determine the temperature distribution over the cross section of the extrudate at the exit. This temperature profile will in turn have an influence on the dimensional uniformity and properties of the product.

In injection molding, a hot molten polymer is injected into a cold cavity. As the polymer comes into contact with the cavity, the skin is frozen and the effective cavity thickness is reduced. The growth of the frozen layer is quite complicated due to the moving front. At the same time the velocity of the polymer and the viscous dissipation increase due to the reduced gap. The temperature distribution in the polymer at the end of the filling phase is extremely complex and has a significant effect on the shrinkage, warpage and residual stresses of the final part as well as the cycle time.

In extrusion blow molding, a hollow polymer cylinder, called a parison, is extruded through an annular die, clamped and inflated by air pressure into a mold to produce hollow parts. During the extrusion process, the parison experiences a non-uniform cooling along its length. The result is a non-uniform modulus which affects the inflation of the parison and the final thickness distribution in the part.

Thus, temperature is probably one of the most important parameters in polymer processing. However, its measurement is extremely difficult, especially its profile in the thickness direction. Previous attempts to measure the temperature profile include using fluorescence spectroscopy [1, 2], ultrasonics [3, 4] and infrared pyrometry [5, 6]. In the fluorescence spectroscopy method, a temperature sensitive dye is incorporated into the polymer at dopant levels and the local temperature is measured by monitoring spectral features of the dye. In the ultrasonic technique, an ultrasonic velocity distribution (tomogram) in a hot body is converted to an internal temperature distribution by employing an inverse method with a precisely measured velocity-temperature relation. In infrared pyrometry, an inverse radiation method, based on the radiant energy emitted by the polymer/boundary system, is used to retrieve the temperature field inside a semi-transparent material. In this work, an inversion technique is developed to predict the temperature distribution in the thickness direction from the surface temperature measurement. The theory is validated using numerically generated data from theoretical temperature profiles developed during polymer flows. The algorithm is then applied to the injection-stretch-blow molding process to predict the temperature distribution in the injection-molded preform before the stretching and inflation phase.

2. Formulation of the inverse problem

The injection-stretch-blow molding (ISBM) process is a very popular method to produce food containers. In the single stage ISBM process, a preform is injection molded, then moved to a blowing station, stretched by a rod to its final length and then inflated. In the two-stage ISBM, the preforms are molded and stored at room temperature until needed. At that point, the preform is reheated in a conditioning oven to an appropriate temperature before stretching and inflation take place. In either case, the temperature distribution in the preform along its length and in its thickness is very important in determining the thickness uniformity of the final part and whether the preform can be stretched and inflated properly [7]. In the following section, the temperature distribution in the thickness of the preform is defined and solved as an inverse problem.

The wall thickness of the preform is usually small compared to its height or width. In this instance, it is reasonable to assume that the heat transfer is one-dimensional. Furthermore, since the temperature of the mold or die is controlled at approximately the same temperature on both sides, the temperature profile is considered symmetric across the mid plane of the thickness. With the above assumptions, the equation governing the temperature evolution in the preform is given by:

$$\rho C_{\mathrm{p}} \frac{\partial T}{\partial t} = \frac{\partial}{\partial x} k \frac{\partial T}{\partial x} \tag{1}$$

with the following boundary and initial conditions:

$$\frac{\partial T}{\partial x} = 0 \quad \text{at} \quad x = 0 \quad \text{(on the plane of symmetry)} \tag{2}$$

$$-k \frac{\partial T}{\partial x} = h(T - T_{\mathrm{a}}) \quad \text{at} \quad x = d \quad \text{(on the surface)} \tag{3}$$

$$T(x, t = 0) = f(x) \tag{4}$$

where T is the temperature, T_{a} the ambient temperature, ρ the density, C_{p} the specific heat, k the thermal conductivity, h the heat transfer coefficient, t and x denote time and spatial coordinate, respectively and d is the half thickness of the part.

If the initial temperature distribution over the thickness of the part were known, the problem is well-posed and a unique solution can be obtained. However, this temperature distribution is usually unknown and difficult to measure. On the other hand, the surface temperature of the part is measurable and is a direct consequence of the internal temperature distribution. The physical definition of this inverse problem is to reconstruct the unknown initial temperature distribution by measuring the surface temperature as a function of time after part ejection. By using different portion of the time response data, the evolution of the temperature profile can be predicted.

Several researchers have considered the inverse heat conduction problem; however, the emphasis has been mainly in the prediction of the surface heat flux under steady or unsteady state conditions, material properties

[8–14] or volumetric heat source [15]. Various techniques have been applied to the solution of such problems including the regularized least square method [9, 16], the sequential estimation [9], the mollification method [18] and the conjugate gradient method using an adjoint equation [8, 13, 15, 18] in conjunction with the finite element method [19] or the boundary element method [20]. In the above works, the initial temperature is assumed known. The prediction of the initial temperature has been relatively ignored [8, 12, 21]. In this work the inverse problem of reconstructing the initial condition of the part across the thickness is formulated using the adjoint method with the resulting equations solved by the finite element technique.

Let the initial condition be given by $f(x)$. If the initial condition is varied by an amount $\Delta f(x)$, the temperature will vary by $\Theta(x,t)$. The function $f(x)$ can be found by minimizing the functional $J[f(x)]$ defined by:

$$J = \int_0^t [T_s(t) - T_m(t)]^2 \, dt \tag{5}$$

where T_s and T_m are, respectively, the computed and the measured surface temperature.

The conjugate gradient method was employed to search for the minimum of the functional. This method has been well documented elsewhere [22, 23] and will not be repeated here. Two quantities needed in this method, the stepsize and the gradient, are obtained by solving the sensitivity problem and the adjoint problem defined as following:

The sensitivity problem

$$\rho C_p \frac{\partial \Theta}{\partial t} = \frac{\partial}{\partial x} k \frac{\partial \Theta}{\partial x} \tag{6}$$

$$\frac{\partial \Theta}{\partial x} = 0 \quad \text{at} \quad x = 0 \tag{7}$$

$$-k \frac{\partial \Theta}{\partial x} = h\Theta \quad \text{at} \quad x = d \tag{8}$$

$$\Theta = \Delta f(x) \quad \text{at} \quad t = 0 \tag{9}$$

where $x = 0$ and $x = d$ denote the plane of symmetry and the part surface, respectively.

The adjoint problem

$$\frac{\partial}{\partial t} \rho C_p \chi + \frac{\partial}{\partial x} k \frac{\partial \chi}{\partial x} + 2(T - T_m)\delta(x - d) = 0 \tag{10}$$

$$\frac{\partial \chi}{\partial x} = 0 \quad \text{at} \quad x = 0 \tag{11}$$

$$-k \frac{\partial \chi}{\partial x} = h\chi \quad \text{at} \quad x = d \tag{12}$$

$$\chi = 0 \quad \text{at} \quad t = t_f. \tag{13}$$

The algorithm for the solution is as follows:

(i) choose an initial guess $T^n(x)$;

(ii) solve the direct problem to obtain the surface temperature $T(d,t)$;

(iii) from the computed $T(d,t)$ and the measured $T_m(t)$, solve the adjoint problem to find the gradient of the functional J

$$J'^n = -(\rho C_p \chi)_{t=0}; \tag{14}$$

(iv) compute the conjugate coefficient by:

$$\gamma^n = \frac{\int_0^d (J'^n(x))^2 \, dx}{\int_0^d (J'^{n-1}(x))^2 \, dx}; \tag{15}$$

(v) calculate the direction of descent:

$$P^n = J'^n + \gamma^n P^{n-1}; \tag{16}$$

(vi) set $\Delta f(x) = P^n$ and solve the sensitivity problem for $\Theta(x,t)$;

(vii) calculate the step size from:

$$\beta^n = \frac{\int_0^{t_f} [T(d,t) - T_m(t)]\Theta(d,t) \, dt}{\int_0^{t_f} [\Theta(d,t)]^2 \, dt} \tag{17}$$

(viii) update the initial guess and repeat the iteration until convergence is achieved:

$$T^{n+1}(x) = T^n - \beta^n P^n. \tag{18}$$

3. Results

In order to test the algorithm, a number of typical temperature profiles developed during polymer flows are considered:

(i) For the fully developed flow of a Newtonian fluid with a temperature-independent viscosity between two parallel isothermal walls, the temperature distribution over the thickness is a fourth order polynomial with a maximum at the centerline [24]. This profile can be emulated by a ramp function consisting of a linear increase followed by a constant as shown in Fig. 2.

(ii) For the developing flow of a Newtonian fluid between two parallel isothermal walls, the temperature profile is characterized by a peak between the centerline and the wall due to the viscous dissipation [25]. This profile is estimated by a triangular temperature shape followed by a constant as depicted in Fig. 3.

(iii) For the coextrusion of two fluids, it is conceivable that each fluid has a constant and different temperature and thus the profile is given by a step function as displayed in Fig. 5.

In the following calculations, a half thickness of 1.5 mm is used since this corresponds to the half thickness

Table 1
Material properties of PET

Density [kg m^{-3}]	1300
Specific heat [J kg^{-1} $°C^{-1}$]	1500 or $1500+4*(T-105)$
Thermal conductivity [W m^{-1} $°C^{-1}$]	0.245
Heat transfer coefficient [W m^{-2} $°C^{-1}$]	15

of the part in the experiments. For each profile, the direct problem was solved to generate the surface temperature using the parameters shown in Table 1. All thermal properties are assumed to be constant unless indicated otherwise. This surface temperature was then used as 'experimental' data to reconstruct the initial temperature profile using the inverse method. The inverse problem is inherently ill-posed, i.e. small errors in the data can incur a large variation in the solution. Since all experimental data contain a certain level of noise, the challenge is to develop a stable algorithm which is less susceptible to noise. To assess the effect of noisy data on the reconstructed temperature profile, a 2% random noise with zero mean was superposed on the exact data. The exact data and those with noise are shown in Fig. 1 for case I. Figure 2 shows a comparison between the input temperature profile and the recovered solutions. When the data are exact, the predicted temperature profile is in excellent agreement with the input except near the sharp corner. This is due to the diffusive nature of the heat equation and the smoothing effect of the inverse algorithm. When the data have a 2% random noise, the

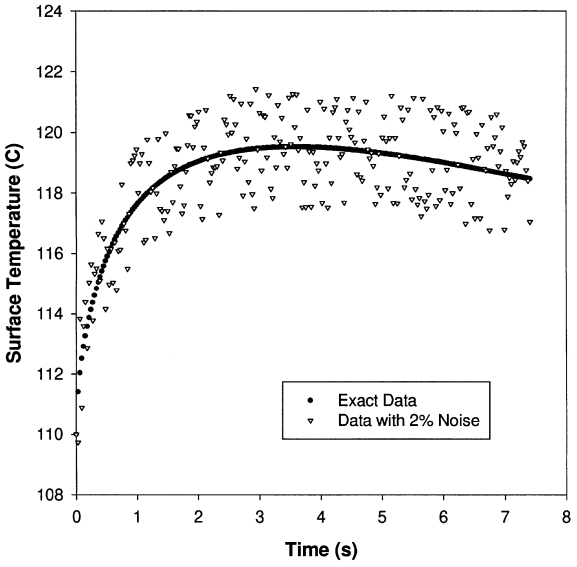

Fig. 1. The surface temperature data generated numerically from an initial ramp function profile shown in Fig. 2.

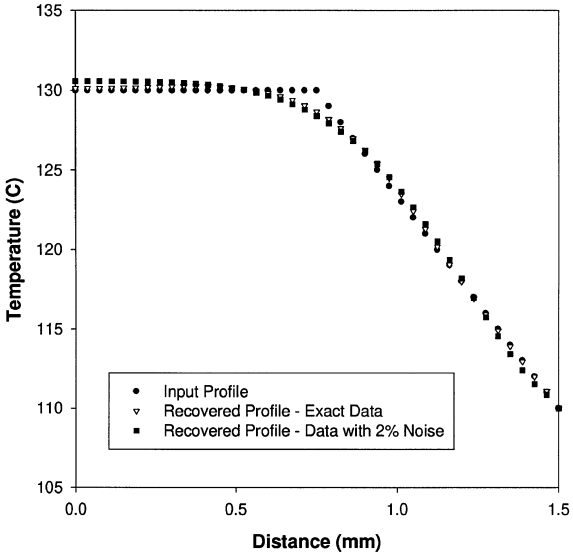

Fig. 2. Comparison between the input initial temperature profile and the reconstructed temperature profiles when the data are exact and when the data contain 2% random noise with zero case. Case 1: ramp function profile.

recovered profile deviates somewhat from the input; however, the error is always less than the noise level and within 2°C even near the sharp corner. This can be considered as very good agreement since it falls within the accuracy of most temperature measurements.

For case II the temperature peak was represented quite well by the inverse solution. The reconstructed temperature is within 2°C of the input profile with exact or noisy data as shown in Fig. 3 except near sharp corners. Similar to the first case, the sharp corners have been rounded by the inverse algorithm. Even though random noise has a zero mean, it may superpose on the data in different sequence from one experiment to another which in turn influences the solution. Noisy data with different sequences were obtained by generating random number series with different seeds. Figure 4a shows the difference between the reconstructed profile obtained using exact data and those obtained with differently seeded noisy data. A 2% noise level results in less than 1% error in the prediction of the initial temperature. The effect of a different noise seed on the predicted surface temperature is even less and confined to the short time response as shown in Fig. 4b. It should be noted that even though the recovered solution is close to the input profile, the position of the maximum temperature is slightly shifted.

For case III, the error is much larger. The step function has been replaced by a smooth sigmoidal function as shown in Fig. 5. Even though two temperature levels can still be visible, the reconstructed temperature can only be

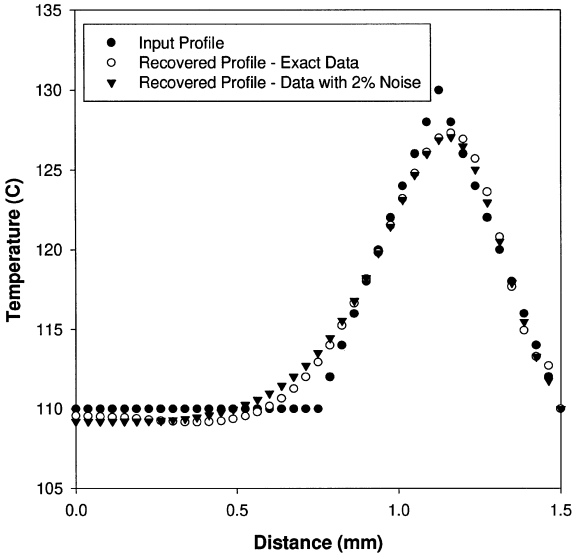

Fig. 3. Comparison between the input initial temperature profile and the reconstructed temperature profiles when the data are exact and when the data contain 2% random noise with zero mean: case 2—triangular temperature profile.

considered as fair. As before, different noise distributions have a negligible effect on the inversion results.

3.1. Effect of error in material properties on the inverse solution

The recovered temperature profile depends not only on the surface temperature but also on the material properties, namely, the density, the specific heat and the thermal conductivity. Another quantity of particular importance is the heat transfer coefficient which depends considerably on the environment and thus can vary from one experiment to another. Their measurements usually involve significant uncertainties. These properties are also temperature dependent giving rise to two difficulties. If the temperature dependence is taken into account, the problem becomes nonlinear. Even though this aspect has been included in the adjoint formulation, the solution is more time consuming. In the range of temperature considered in this work, the temperature dependence is rather weak and the thermal properties are assumed to be constant, giving rise to a certain error in the solution. In the following sections, the effect of the variation in material properties on the inversion will be examined to determine the resulting error level.

The surface temperature data for case I were generated using the material properties given in Table 2. The inverse solution is now obtained using different thermal properties. Figure 6 shows the effect of a 20% change in specific heat on the recovered temperature profile. In Fig. 7, com-

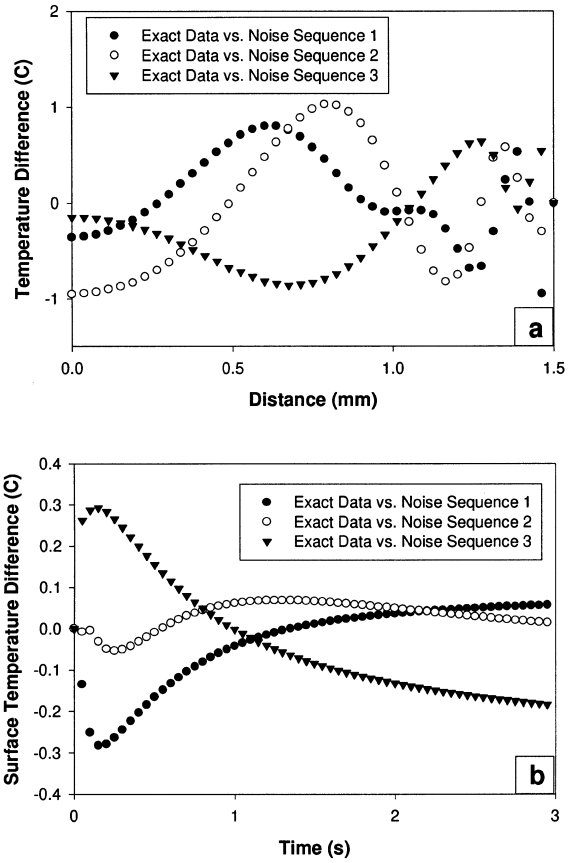

Fig. 4. The effect of different noise sequence on the recovered initial temperature profile and the predicted surface temperature: (a) the difference between the initial profile identified with exact data and those with noisy data; (b) the difference between predicted surface temperature using exact data and those with noisy data.

parison is made between three different values of thermal conductivity, namely, 0.200, 0.245 and 0.300 $W\,m^{-1}\,K^{-1}$ which represents about $\pm 20\%$ change with respect to the measured value of 0.245. The 20% variation in thermal properties is considerably larger than the uncertainty of less than 10% incurred in most measurements [26, 27]. Even with such large changes in thermal properties, the predicted temperature profile is still quite reproducible. The variation in thermal properties has a larger effect at longer time which is reflected in the temperature recovery near the center line.

One of the most difficult parameters to measure is the heat transfer coefficient. In Fig. 8, the heat transfer coefficient was changed by $\pm 30\%$. The profile near the surface still shows a remarkable resemblance to the input profile while near the center a maximum of 5°C variation is obtained. The predicted surface temperature is very close to the input data (within 0.2%) indicating that the

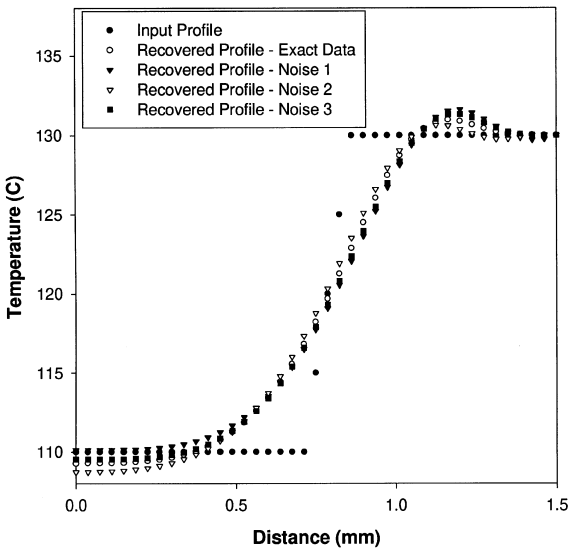

Fig. 5. Comparison between the input initial temperature profile and the reconstructed temperature profiles when the data are exact and when the data contain 2% random noise having different distribution: case 3—step function profile.

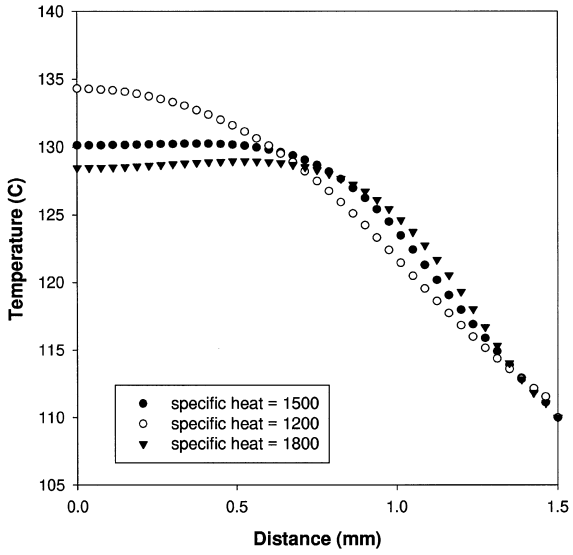

Fig. 6. The effect of error in specific heat on the reconstructed initial temperature profile.

Table 2
Injection molding conditions

Melt temperature [°C]	270
Mold temperature [°C]	20
Ambient temperature [°C]	25
Injection time [s]	1
Cycle time [s]	6

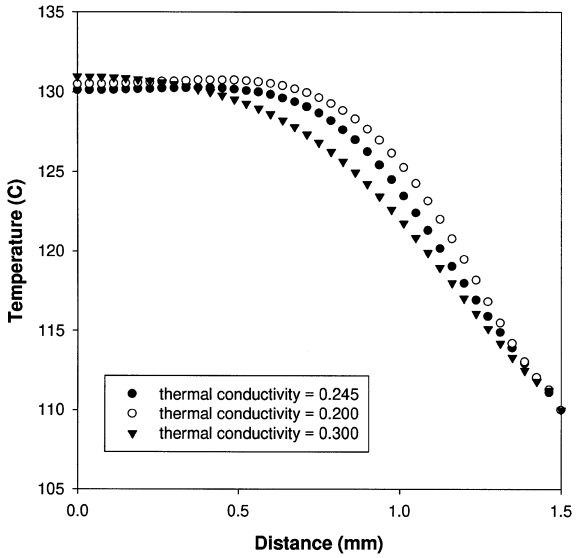

Fig. 7. The effect of error in thermal conductivity on the reconstructed initial temperature profile.

fit is very good. However, when the two recovered profiles were used to predict the surface temperature at longer times, larger deviation was obtained as shown in Fig. 9. Therefore, for a given set of surface temperature data, a portion of the data can be used to identify the initial profile and the rest of the data may be used in an iterative procedure to predict the heat transfer coefficient, or in general, the thermal properties of the materials. One of the difficulties in this procedure is to choose the appropriate portion of the data to be used for the reconstruction of the initial profile. In this work, the minimum amount of data required in terms of time is estimated by equation (19) based on the transient heat conduction in a semi-infinite medium:

$$\tau = \frac{d^2}{4\alpha} \tag{19}$$

where $\alpha = k/\rho C_p$ is the diffusivity of the material and d is the half thickness of the part. This procedure has been used to obtain the value of heat transfer coefficient given in Table 1 and used throughout this work.

4. Experimental

In this work, the experiments were carried out in a single stage AOKI injection-stretch-blow molding machine. The material employed is a blow molding grade

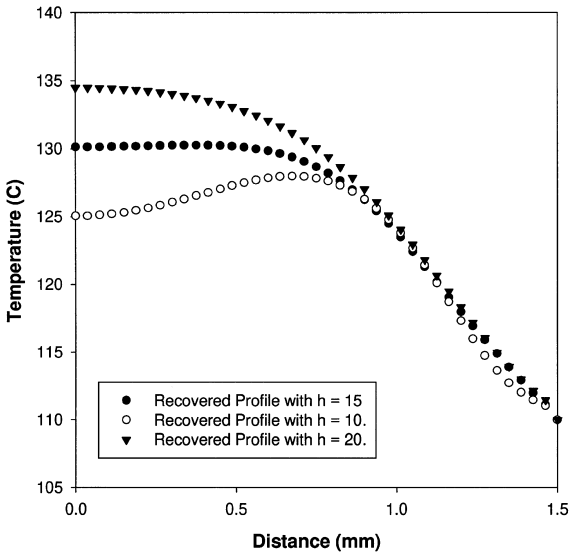

Fig. 8. The effect of error in heat transfer coefficient on the reconstructed initial temperature profile.

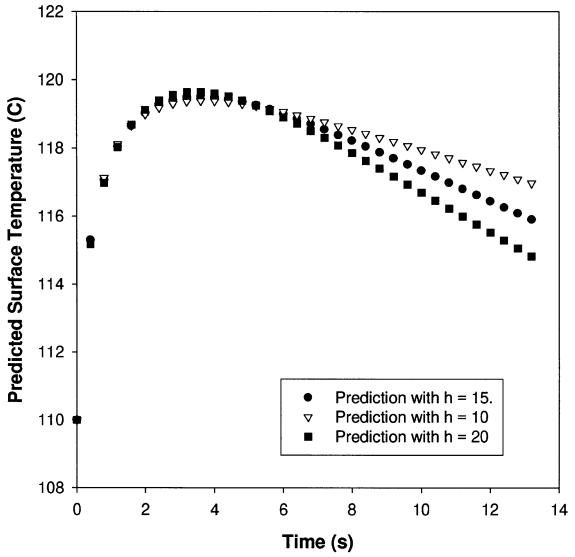

Fig. 9. The effect of error in heat transfer coefficient on the predicted surface temperature at longer time.

Polyethylene Terephthalate (Kodapak 9921). The material properties and the injection molding conditions are given in Tables 1 and 2, respectively. The heat transfer coefficient is included in Table 1 even though it is not strictly a material property. Its measurement is rather difficult and thus it is estimated by a trial and error procedure to be explained later. An infrared camera (AGEMA 900, 8–12 μm wavelength) was used to record the surface temperature of the preform as it was taken out of the injection mold and held in place at the thread region. The thickness of the preform is about 3 mm. The material is transparent to visible light during the measurement but it is opaque to infrared light with a penetration depth of the order of 50 μm. To ensure that the measured temperature is the surface temperature, a narrow wavelength filter centered at 8.93 μm was also used. During the molding of the preform, a hot polymer melt at 270°C is injected into the cold cavity at about 20°C. While inside the cavity, the packing pressure keeps the polymer in contact with the mold resulting in a cold surface and a hot interior. When the preform is removed from the mold, which corresponds to time $t = 0$ in the experiments, heat from the hot interior moves to the surface causing the temperature to rise. A picture of the preform and a typical surface temperature–time plot are shown in Figs 10 and 11.

The inverse algorithm is now applied to the surface temperature data obtained from the infrared camera. Figure 12 shows the predicted temperature profile across the thickness of the preform from the centerline to the surface. The predicted profile shows a maximum at the center which is due to the high melt temperature. A shoulder is apparent about 0.5 mm from the surface. This could arise from heat generation by viscous dissipation during the filling, but it could also be due to the oscillation from the algorithm. This point is very difficult to evaluate without a direct method to measure the temperature. Since the thermal conductivity of PET remains essentially unchanged in the temperature range of the experiments (70–180°C), only the effect of variable specific heat is examined. Two constant specific heat values are considered: a low value of 1500 J kg^{-1} $°C^{-1}$ and a high value of 1800 J kg^{-1} $°C^{-1}$ which are the estimated specific heat of PET at temperatures on the surface and in the center, respectively. The change in specific heat with temperature is also fully accounted for using a linear function given in Table 1. The reconstructed profiles show a lowest temperature in the center for the highest value of specific heat while it is highest for the case of variable specific heat. The temperature profile near the surface is practically the same for all three cases. The difference between the profiles obtained using the specific heat of 1500 J kg^{-1} $°C^{-1}$ is quite comparable to that obtained with a variable specific heat model. Thus, even though it has been shown that the inversion technique can provide a fairly reliable temperature prediction within a few percent, caution should be taken not to overinterpret the results. Since the glass transition temperature of PET is about 70°C, this profile confirms that the preform is still in the rubbery zone and thus can be deformed easily during the blowing stage. A very good agreement can be achieved between the predicted surface temperature using this profile and the experimental data as presented in Fig. 11. This indicates that the minimization algorithm is quite adequate for the problem at hand.

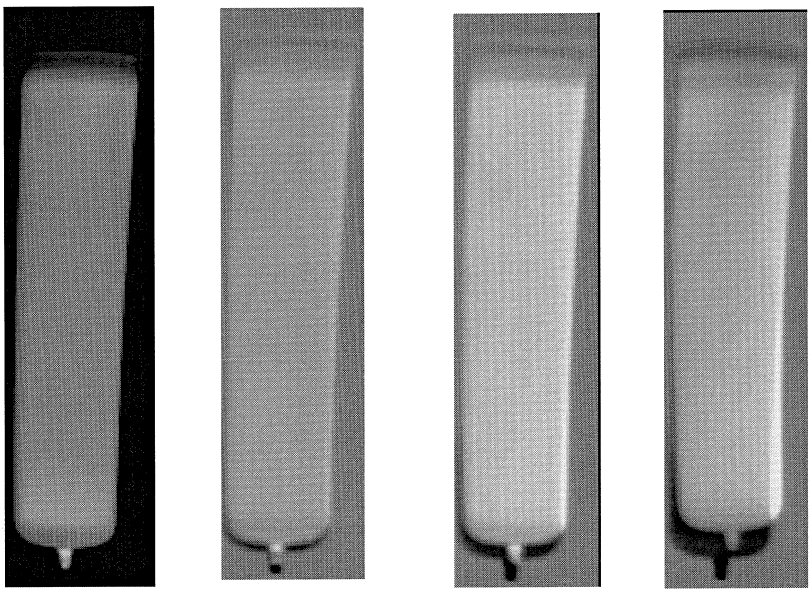

Fig. 10. The shape of the preform as it was taken out of the injection mold and held in place at the thread region. The four pictures show the evolution of the surface temperature with time.

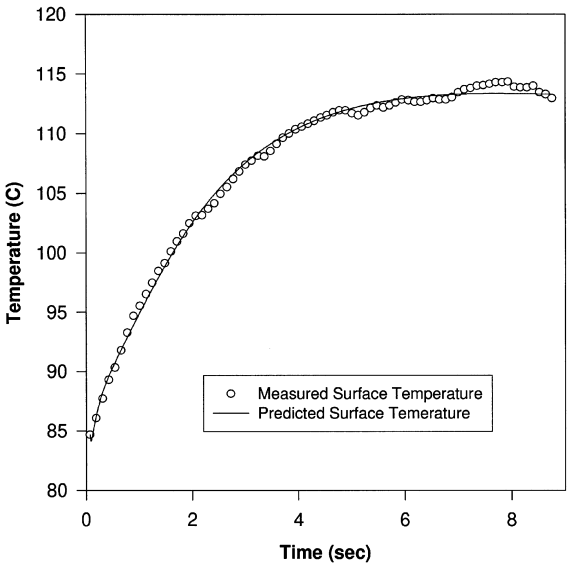

Fig. 11. A typical plot of the measured temperature vs time at one point on the surface of the preform and comparison with the predicted temperature.

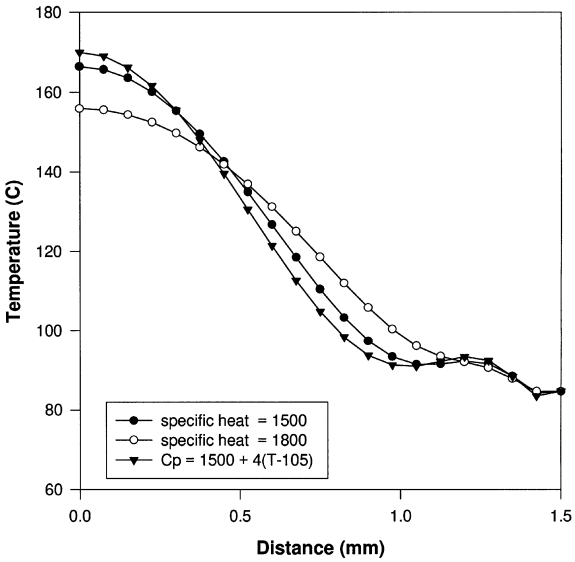

Fig. 12. The temperature profile over the thickness of the preform when it was just taken out of the injection mold as reconstructed using the data shown in Fig. 11 and different specific heat values.

The heat transfer coefficient h was estimated by a trial and error method. Using the measured surface temperature over a short time segment $0 < t < \tau$, the initial temperature profile is predicted. This profile is then used to calculate the 'extrapolated' surface temperature, i.e. the surface temperature for longer time $t > \tau$. From the half thickness of the preform (about 1.5 mm) and the material properties of PET as given in Table 1, τ is estimated to be 4.5 s. As shown in Section 3.1, this 'extrapolated' surface temperature tends to deviate from the measured temperature if an incorrect value of heat transfer coefficient was used. The heat transfer coefficient h is adjusted and a new 'extrapolated' surface temperature is

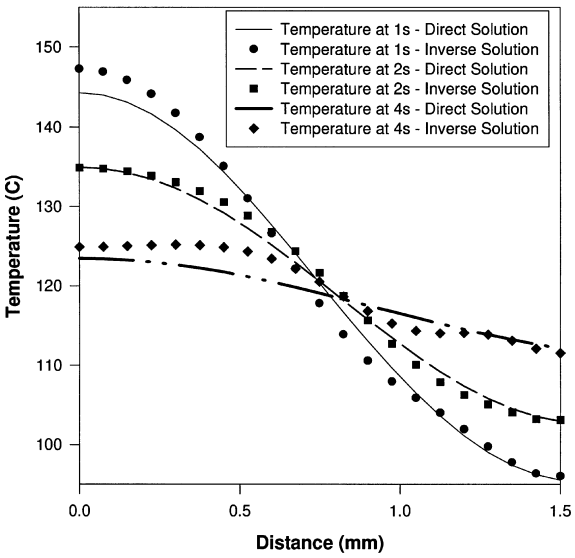

Fig. 13. Comparison of the temperature distribution in the thickness of the preform as predicted by the forward solution and the inverse solution at different times after taken out of the injection mold.

calculated until it matches with the measured temperature. This estimated value of heat transfer coefficient is of the same order of magnitude as those reported in the literature for free convection in air [23] and thus is adopted for all other calculations.

To obtain the temperature profile in the preform at any time after ejection, two methods were used. In one method, the predicted initial profile was used in the direct problem. In the other method, the experimental data at later times, i.e. the data from 1, 2 or 4 s to the end, were used in the inversion. In the direct problem, the initial profile identified using the specific heat value of 1500 J $kg^{-1}\,^{\circ}C^{-1}$ is used. Figure 13 shows a very good agreement between the profiles obtained by the two methods indicating that the inversion algorithm is quite consistent and reliable. The prediction of the temperature profile in the thickness direction with time can be used to optimize the molding process. This is the subject of on-going research.

5. Conclusions

An inversion algorithm was developed to reconstruct the initial temperature from the surface temperature data. The method was validated using exact data generated numerically and showed excellent agreement even with addition of 2% random noise. It was then applied to predict the internal temperature profile of an injection molded preform used in the injection-stretch-blow molding process. A reasonable profile was obtained which needs to be verified by other method. The heat transfer coefficient has also been identified which is in agreement with values reported in the literature. Even though it was shown that the inversion technique can provide a fairly reliable temperature prediction within a few percent, caution should be taken not to overinterpret the results, especially small scale details.

Acknowledgement

The authors would like to thank Mr Christian de Grandpré for carrying out the molding experiments.

References

[1] A.J. Bur, F.W. Wang, C.L. Thomas, J.L. Rose, In-line optical monitoring of polymer injection molding, Poly. Eng. Sci. 34 (1994) 671–679.
[2] K.B. Migler, A.J. Bur, Fluorescence based measurement of temperature profiles during polymer processing, Poly. Eng. Sci. 38 (1998) 213–221.
[3] M. Konno, A. Cui, N. Nishiwaki, S. Hori, Measurement of the polymer melt temperature in injection molding machine by using ultrasonic technique, in: Proceedings of the 51st Annual Technical Conference, Society of Plastics Engineers, New Orleans, 1993, pp. 2798–2803.
[4] H.N.G. Wadley, S.J. Norton, F. Mauer, B. Droney, Ultrasonic measurement of internal temperature distribution, Phil. Trans. R. Soc. London A320 (1986) 341–361.
[5] J.X. Rietveld, G.Y. Lai, Inverse method for obtaining the temperature profile within a mold via IR pyrometry, in: Proceedings of the 52nd Annual Technical Conference, Society of Plastics Engineers, San Francisco, 1994, pp. 836–841.
[6] G.Y. Lai, J.X. Rietveld, Role of polymer transparency and temperature gradients in the quantitative measurement of process stream temperature during injection molding via IR pyrometry, Poly. Eng. Sci. 36 (1996) 1755–1768.
[7] D.V. Rosato, D.V. Rosato (Eds.), The Blow Molding Handbook, Hanser, Munich, 1989.
[8] O.M. Alifanov, Inverse Heat Transfer Problems, Springer-Verlag, Berlin, 1994.
[9] J.V. Beck, B. Blackwell, C.R. St Clair, Jr., Inverse Heat Conduction, John Wiley and Sons, New York, 1985.
[10] R.G. Hills, E. Hensel, One-dimensional nonlinear inverse heat conduction technique, Numer. Heat Transfer 10 (1986) 369–393.
[11] B. Sawaf, M.N. Ozisik, Y. Jarny, An inverse analysis to estimate linearly temperature dependent thermal conductivity components and heat capacity of an orthotropic medium, Int. J. Heat Mass Transfer 38 (1995) 3005–3010.
[12] D.A. Murio, D. Hinestroza, The space marching solution of the inverse heat conduction problem and the identification of the initial temperature distribution, Comp. Math. Applic. 25 (1993) 55–63.
[13] C.H. Huang, M.N. Ozisik, B. Sawaf, Conjugate gradient method for determining unknown contact conductance

during metal casting, Int. J. Heat Mass Transfer 35 (1992) 1779–1986.
[14] C.H. Huang, J.-Y. Yan, An inverse problem in simultaneously measuring temperature-dependent thermal conductivity and heat capacity, Int. J. Heat Mass Transfer 38 (1995) 3433–3441.
[15] A.J. Silva Neto, M.N. Ozisik, The estimation of space and time dependent strength of a volumetric heat source in a one-dimensional plate, Int. J. Heat Mass Transfer 37 (1994) 909–915.
[16] A.N. Tikhonov, V.Y. Arsenin, Solutions of Ill-posed Problems, Winston, Washington, DC, 1977.
[17] D.A. Murio, The mollification method and the numerical solution of the inverse heat conduction problem by finite differences, Comp. Math. Applic. 17 (1989) 1385–1396.
[18] Y. Jarny, M.N. Ozisik, J.P. Bardon, A general optimization method using adjoint equation for solving multi-dimensional inverse heat conduction, Int. J. Heat Mass Transfer 34 (1991) 2911–2919.
[19] R.G. Keanini, N.N. Desai, Inverse finite element reduced mesh method for predicting multi-dimensional phase change boundaries and nonlinear solid phase heat transfer, Int. J. Heat Mass Transfer 39 (1996) 1039–1049.
[20] D.B. Ingham, Y. Yuan, Boundary element solutions of the steady state, singular inverse heat transfer equation, Int. J. Heat Mass Transfer 37 (Supp. 1) (1994) 273–280.
[21] S. Quilliet, Ph. Lebot, D. Delaunay, Y. Jarny, Heat transfer at the polymer–metal interface—a method of analysis and its application to injection molding, in: ASME Proceedings of the 32nd National Heat Transfer Conference, vol. 2, 1997, pp. 9–16.
[22] W.H. Press, S.A. Teukolsky, W.T. Vetterling, B.P. Flannery, Numerical Recipes in FORTRAN: The Art of Scientific Computing, Cambridge University Press, New York, 1992.
[23] G.H. Golub, C.F. Van Loan, Matrix Computations, 2nd ed., Johns Hopkins University Press, Baltimore, 1989, p. 519.
[24] R.B. Bird, W.E. Stewart, E.N. Lightfoot, Transport Phenomena, Wiley, New York, 1960.
[25] R.B. Bird, R.C. Armstrong, O. Hassager, Dynamics of Polymeric Liquids, vol. 1, Fluid Mechanics, 2nd ed., Wiley, New York, 1987.
[26] Annual Book of ASTM Standards, vol. 14.02, Standard E1269-94, American Society for Testing and Materials, Philadelphia, 1995, pp. 797–801.
[27] H. Lobo, C. Cohen, Measurement of thermal conductivity of polymer melts by the line source method, Poly. Eng. Sci. 30 (1990) 65–70.